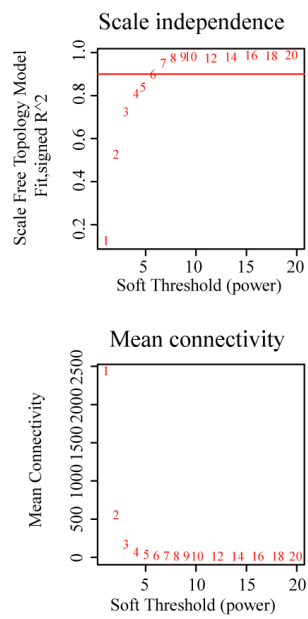


A



B

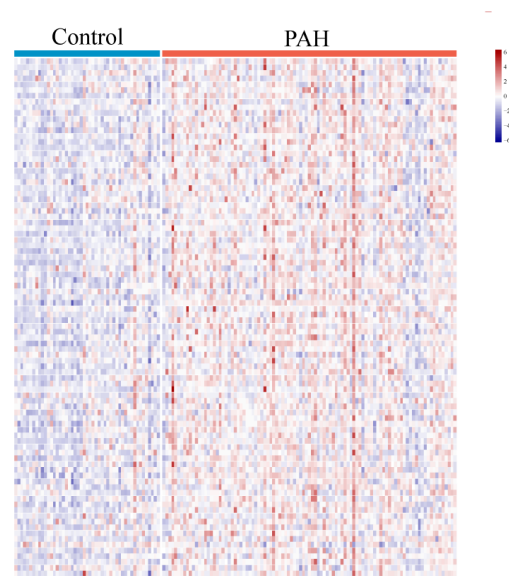


Figure S1. The module detection by WGCNA. (A) In the scale-free topology plot, the up panel shows the scale-free index as a function of the soft thresholding power. The down panel displays the mean connectivity as a function of the soft-thresholding power. (B) The heat map of the white gene expression between normal lungs and PAH lungs. WGCNA, weighted gene co-expression network analysis; PAH, pulmonary arterial hypertension.

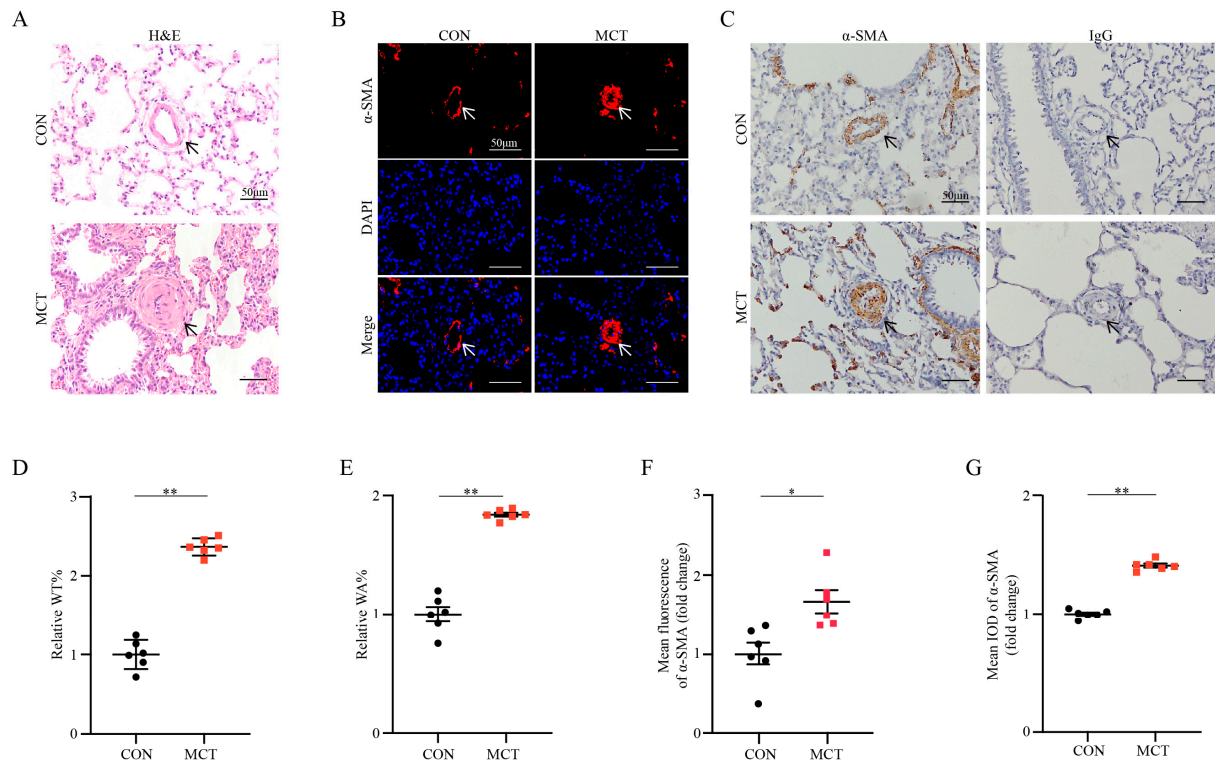


Figure S2. H&E staining and immunohistochemical staining of rat pulmonary artery. (A) Representative images of H&E staining in the pulmonary artery of CON and PAH rats (n=6; scale bar, 50 μm). (B) Representative images of immunofluorescence staining in the pulmonary artery of CON and PAH rats (n=6; scale bar, 50 μm). (C) Representative images of immunohistochemical staining in the pulmonary artery of CON and PAH rats (n=6; scale bar, 50 μm). (D, E) Quantitative analysis of WT% and WA% of pulmonary artery of H&E staining (n=6 each). (F) Representative immunofluorescence staining quantification of α-SMA. (G) Representative immunohistochemical quantification of α-SMA. Data are shown as mean ± SEM. * $p < 0.05$, ** $p < 0.01$ vs. CON group (student's t -test). CON, control rats without pulmonary arterial hypertension; PAH, pulmonary arterial hypertension; MCT, monocrotaline; H&E, hematoxylin eosin; WT%, (the diameter of external vessel – the diameter of internal vessel) / the diameter of external vessel × 100%; WA%, (the total area of the vessel – the lumen area of the vessel) / the total area of vessel × 100%; IOD, the integral optical density; α-SMA, α-smooth muscle actin. The black/white arrow represents pulmonary artery.

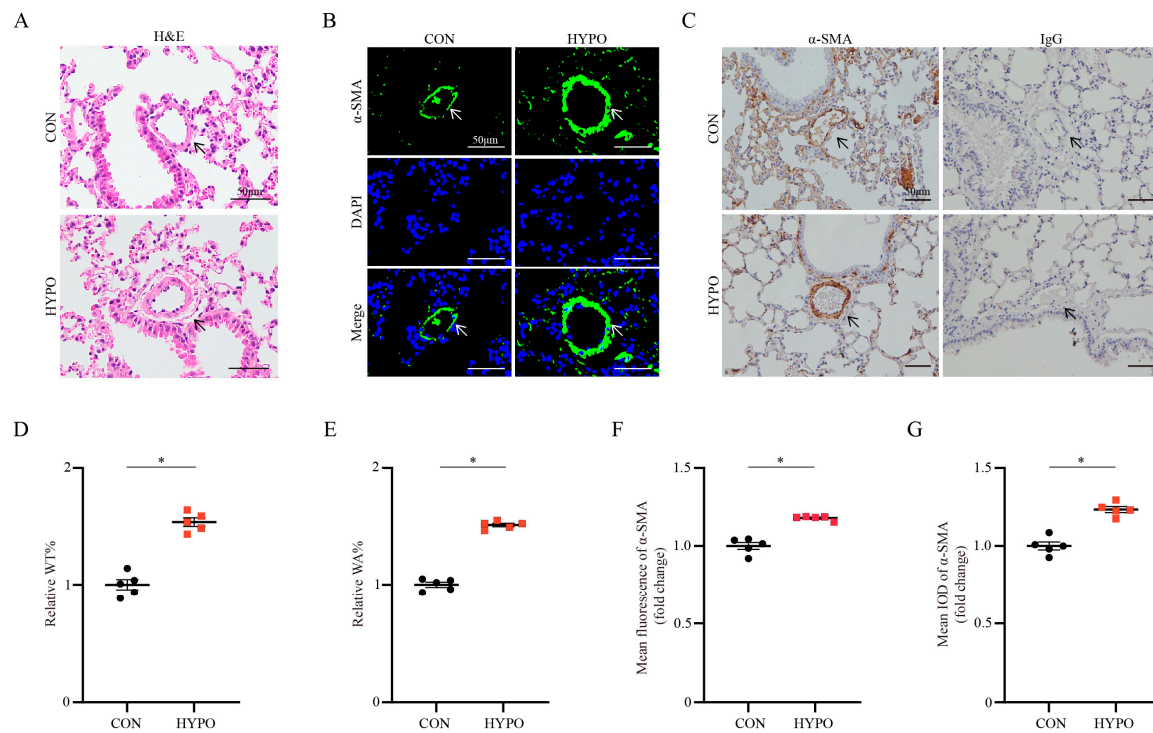


Figure S3. H&E staining and immunohistochemical staining of mouse pulmonary artery. (A) Representative images of H&E staining in the pulmonary artery of CON and PAH mice (n=5; scale bar, 50 μ m). (B) Representative images of immunofluorescence staining in the pulmonary artery of CON and PAH mice (n=5; scale bar, 50 μ m). (C) Representative images of immunohistochemical staining in the pulmonary artery of CON and PAH mice (n=5; scale bar, 50 μ m). (D, E) Quantitative analysis of WT% and WA% of pulmonary artery of H&E staining (n=5 each). (F) Representative immunofluorescence staining quantification of α -SMA. (G) Representative immunohistochemical quantification of α -SMA. Data are shown as mean \pm SEM. * p < 0.05 vs. CON group (student t-test). CON, control mice without pulmonary arterial hypertension; PAH, pulmonary arterial hypertension; HYPO, hypoxia; H&E, hematoxylin eosin; WT%, (the diameter of external vessel – the diameter of internal vessel) / the diameter of external vessel \times 100%; WA%, (the total area of the vessel – the lumen area of the vessel) / the total area of vessel \times 100%; IOD, the integral optical density; α -SMA, α -smooth muscle actin. The black/white arrow represents pulmonary artery.

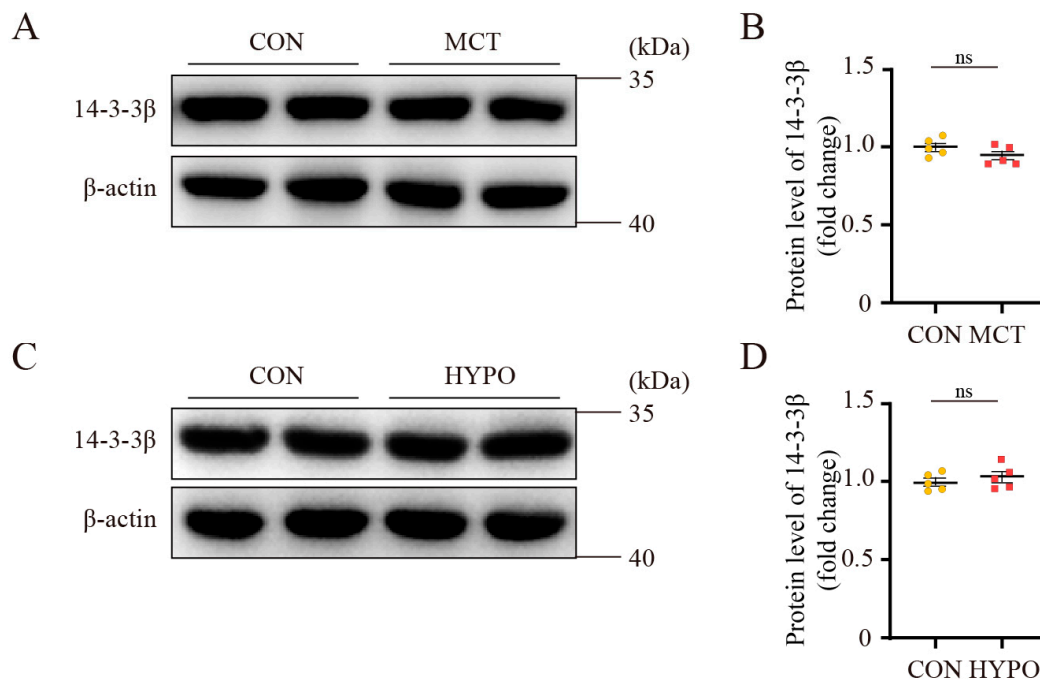


Figure S4. Representative Western blots and analysis of 14-3-3 β expression in rat/mouse lung. (A, B) Representative images of Western blots of 14-3-3 β expression in rat lung. (C, D) Representative images of Western blots of 14-3-3 β expression in mouse lung. Equal protein loading was confirmed using an anti- β -actin antibody (n=5 each). Data are shown as mean \pm SEM (n=5 each); ns represents statically non-significant (student's *t*-test).

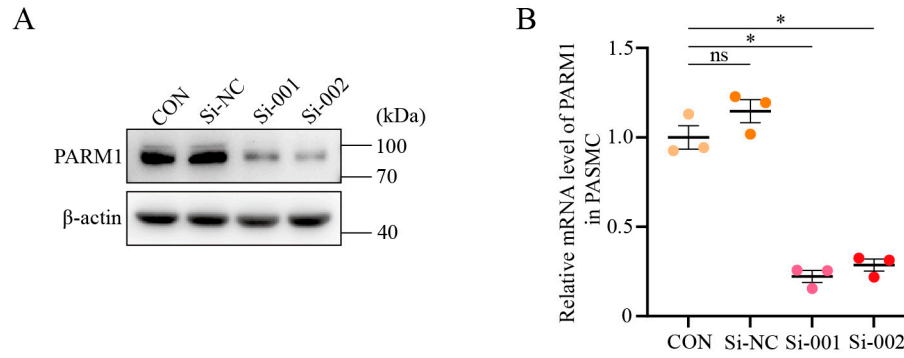


Figure S5. Validation of PARM1 siRNAs in PASC. Different siRNA of PARM1, Si-001 and Si-002, as well as scrambled control, Si-NC were tested in primarily isolated PASC. Representative Western blots (A) and qPCR results as summarized in a dot plot (B) showed that both siRNAs could significantly downregulate the expression of PARM1 in PASC. Data are shown as mean \pm SEM ($n=3$); ns represents statically non-significant. $*p < 0.05$ vs. CON group (student's t -test).